frontiers | Frontiers in Oncology

TYPE Original Research
PUBLISHED 08 January 2024
DOI 10.3389/fonc.2023.1325105

OPEN ACCESS

EDITED BY
Susanne Rogers,
Aarau Cantonal Hospital, Switzerland

REVIEWED BY
Paul Riviere,
University of California, San Diego, United States
Yoichi Watanabe,
University of Minnesota Twin Cities, United States

*CORRESPONDENCE
Jeffrey Snyder
Jeffrey-snyder@uiowa.edu

RECEIVED 20 October 2023
ACCEPTED 18 December 2023
PUBLISHED 08 January 2024

CITATION
Snyder J, Smith B, Aubin JS, Shepard A and Hyer D (2024) Simulating an intra-fraction adaptive workflow to enable PTV margin reduction in MRIgART volumetric modulated arc therapy for prostate SBRT.
Front. Oncol. 13:1325105.
doi: 10.3389/fonc.2023.1325105

Simulating an intra-fraction adaptive workflow to enable PTV margin reduction in MRIgART volumetric modulated arc therapy for prostate SBRT

Jeffrey Snyder*, Blake Smith, Joel St. Aubin, Andrew Shepard and Daniel Hyer

Department of Radiation Oncology, University of Iowa Hospitals and Clinics, Iowa City, IA, United States

Purpose: This study simulates a novel prostate SBRT intra-fraction re-optimization workflow in MRIgART to account for prostate intra-fraction motion and evaluates the dosimetric benefit of reducing PTV margins.

Materials and methods: VMAT prostate SBRT treatment plans were created for 10 patients using two different PTV margins, one with a 5 mm margin except 3 mm posteriorly (standard) and another using uniform 2 mm margins (reduced). All plans were prescribed to 36.25 Gy in 5 fractions and adapted onto each daily MRI dataset. An intra-fraction adaptive workflow was simulated for the reduced margin group by synchronizing the radiation delivery with target position from cine MRI imaging. Intra-fraction delivered dose was reconstructed and prostate DVH metrics were evaluated under three conditions for the reduced margin plans: Without motion compensation (no-adapt), with a single adapt prior to treatment (ATP), and lastly for intra-fraction re-optimization during delivery (intra). Bladder and rectum DVH metrics were compared between the standard and reduced margin plans.

Results: As expected, rectum V18 Gy was reduced by 4.4 ± 3.9%, D1cc was reduced by 12.2 ± 6.8% (3.4 ± 2.3 Gy), while bladder reductions were 7.8 ± 5.6% for V18 Gy, and 9.6 ± 7.3% (3.4 ± 2.5 Gy) for D1cc for the reduced margin reference plans compared to the standard PTV margin. For the intrafraction replanning approach, average intra-fraction optimization times were 40.0 ± 2.9 seconds, less than the time to deliver one of the four VMAT arcs (104.4 ± 9.3 seconds) used for treatment delivery. When accounting for intra-fraction motion, prostate V36.25 Gy was on average 96.5 ± 4.0%, 99.1 ± 1.3%, and 99.6 ± 0.4 for the non-adapt, ATP, and intra-adapt groups, respectively. The minimum dose received by the prostate was less than 95% of the prescription dose in 84%, 36%, and 10% of fractions, for the non-adapt, ATP, and intra-adapt groups, respectively.

Conclusions: Intra-fraction re-optimization improves prostate coverage, specifically the minimum dose to the prostate, and enables PTV margin reduction and subsequent OAR sparing. Fast re-optimizations enable uninterrupted treatment delivery.

KEYWORDS

VMAT (volumetric modulated arc therapy), intra-fraction, MRIgRT, adaptive, tracking, prostate SBRT treatment, MR-linac

1 Introduction

Prostate cancer is the second most prevalent type of cancer among men in the United States with an estimated 288,300 newly diagnosed cases in 2023 (1). Radiation therapy has an important role in the treatment of prostate cancer with an estimated 60% of patients requiring radiation therapy at some point over the course of their disease (2, 3). Treatments have proven to be very effective as evidenced by the 99% overall survival rate at 10 years for patients who have localized disease and who are diagnosed at early stage with low to intermediate risk of recurrence (4).

Studies have shown that the prostate has a low alpha/beta ratio of approximately 1.5 while nearby critical organs at risk (OAR) such as the bladder and rectum have alpha over beta ratios in the range of 3 -5 Gy for late toxic effects (5–9). These radiobiological factors indicate that the prostate is sensitive to high dose per fraction treatments. This makes prostate SBRT an attractive treatment option which has now become an increasingly used treatment method (10). Clinical trials comparing survival and toxicity profiles have shown non-inferiority for SBRT as compared to conventional fractionation in the treatment of prostate cancer (11–13). SBRT also reduces the number of fractions which improves patient satisfaction and is a more cost-effective treatment as compared to conventional fractionation (5, 14–16). While these are positive factors and the toxicity rate for prostate SBRT is generally considered acceptable, side effects remain. Alongi et al. reported a 40% incidence of grade 2 Genito-urinary (GU) toxicities while Kishan et al. reported a 10% incidence of grade 2 or greater gastrointestinal (GI) toxicity (17, 18). With a high overall survival rate, a focus on developing treatment strategies which reduce side effects should remain a priority.

One method which will better spare OAR's and potentially reduce treatment related side effects is the reduction of PTV margins (19). Reducing PTV margins poses challenges as the prostate exhibits both inter and intra-fraction motion caused by bladder and rectal filling, bowel movement, and skeletal muscular motion (20–22). Therefore, caution should be employed when implementing margin reductions because advanced imaging technologies and strategies may be required to prevent underdosage of the target (23, 24). Prostate PTV margins ranging from 2 mm to greater than 10 mm have been reported in the literature and this variation often coincides with the type of pretreatment imaging used and whether intra-fraction adaptions are applied (25). Most commonly, PTV margins fall within the range of 4 to 6 mm (22, 26–28). Keizer et al. found that PTV margin reduction below 4 mm would require intra-fraction monitoring and correction (29). Common intra-fraction monitoring techniques used in prostate radiotherapy include the use of triggered planar imaging of implanted fiducials or through electromagnetic tracking of implanted beacons (30–33). While these methods aid in monitoring and correcting intra-fraction motion, they have drawbacks including an invasive seed implantation and an extra appointment for the patient (34). Additionally, triggered imaging methodologies add additional non-target specific ionizing radiation, and electromagnetic beacons cause artifacts limiting the use of MRI in delineation of the prostate (31, 35). Lastly, these intra-fraction correction methods can add additional treatment time. Gorovets et al. reported a maximum fractional treatment time of 45 minutes when monitoring with kV/MV imaging on a standard linear accelerator and implementing a 2 mm correction threshold (36). Furthermore, Kisivan et al. reported that 29% of treatment fractions would require greater than 1 intra-fraction intervention when using a 3 mm motion threshold (37).

MRI guided adaptive radiotherapy (MRIgART) has emerged as a promising technique for treating prostate cancer. MRIgART enables real time cine imaging and target tracking without additional ionizing radiation or fiducial markers (38, 39). It is estimated that one third of prostate patients require adaptive radiotherapy which can be applied online with MRIgART (40). The MIRAGE trial compared non-adaptive MRI linac based treatments using reduced margins versus treatments delivered with conventional linacs and standard margins, finding that MRI guided radiotherapy reduced GU and GI toxicities (18). Additionally, in a meta-analysis of 29 prospective studies, Leeman et al. found that MRI guided radiotherapy reduced urinary side effects by 44% and bowel side effects by 60% as compared to conventional CT guided treatment methods with implanted fiducials (41). Combining reduced PTV margins and online adaptive re-planning may further reduce treatment related toxicities. However, long treatment session times associated with MRIgART and intra-fraction motion limit the extent to which PTV margins can be reduced without intra-fraction compensation (29,

42, 43). MRIgART with daily re-planning commonly uses prostate PTV margins ranging between 3 and 5 mm (44–48) with 5 mm in all directions except for 3 mm in the posterior direction remaining a standard (43, 49–51). While techniques such as gating and/or baseline shift corrections can be used in conjunction with reduced PTV margins, this will add additional time to already long treatment sessions and therefore is impractical for some patients (42, 43). This may be especially impactful on systems such as the Elekta Unity which does not support couch movement during treatment and thus, users must wait for baseline shift plans to be re-optimized or re-calculated prior to resuming treatment if target excursions occur (52, 53).

Recently, the use of 2D cine MRI imaging coupled with target tracking has been used to reconstruct the fractional dose delivered to the target for prostate and seminal vesicle treatments (29, 48, 54). Additionally, the feasibility of VMAT treatment delivery techniques have been shown which reduce delivery time as compared to step-and-shoot IMRT, the current standard for all MRI-linacs (55, 56). This study builds on these earlier works by simulating a novel intra-fraction MRIgART workflow that combines cine MRI target tracking and VMAT delivery to enable intra-fraction dose re-optimization without causing delays in treatment. The efficacy of the workflow to maintain adequate prostate coverage with 2 mm PTV margins while accounting for intra-fraction motion was also evaluated.

2 Materials and methods

2.1 Patient selection and reference planning

Ten prostate cancer patients previously treated on our Elekta Unity MRI linac were enrolled in this retrospective planning study. All patients provided informed prospective consent to use their treatment images and this study was conducted in accordance with the International Council for Harmonization ICH E6 (R2) Good Clinical Practice as adopted by the United States FDA, which aligns with the principles of Helsinki. Each patient received a simulation CT scan with 2 mm slice thickness as well as a diagnostic T2 MRI image to aid in the delineation of the prostate. In this study, all patients were simulated to be low risk prostate cancer patients without seminal vesicle or nodal involvement. A SpaceOAR hydrogel spacer was placed for all patients except for patient 7 who declined. The SpaceOAR increases the separation between the prostate and rectum and aids in the reduction of rectal dose (57). The gross tumor volume consisted of the prostate and no additional expansion was used for the CTV (GTV = CTV). A research Monaco treatment planning system (version 6.09.00) was used to generate reference MRIgART VMAT treatment plans using two separate PTV margins. The standard PTV margin group consisted of a 5 mm expansion of the CTV in all directions except for 3 mm posteriorly, while the reduced PTV margin group used a uniform 2 mm expansion of the CTV. A previously commissioned clinical beam model was used to generate all plans within this study (52). For this study, all plans were optimized to deliver 36.25 Gy in 5 treatment sessions and normalized for 95% PTV coverage. OAR dose limits for planning followed our institutional standard which is based off of the criteria published by the PACE B clinical trial and Tanaka et al. (26, 58).

2.2 Cine MRI target tracking

Cine MRI images were acquired during radiation delivery for each fraction and all patients enrolled in this study. The cine MRI consisted of a balanced T1/T2 fast spin echo (TE 3.8 ms, TR 1.92 ms, flip angle: 40 degrees) imaging sequence which comes standard on the Unity system (59). The cine MRI sequence had temporal resolution of 200 msec with coronal and sagittal images being acquired in an interleaved fashion. The pixel size of the cine MRI images was 1.13 mm with a 5 mm slice thickness (60).

A preclinical motion management research package (MMRP) was used to retrospectively analyze and track the position of the prostate in each frame of the cine MRI acquisitions. Details of the target tracking algorithm have been previously published (39, 60, 61). Briefly, the algorithm begins by using 2D-3D template matching. In this stage the first 60 cine MRI images (30 sagittal and 30 coronal) are used to generate a single average 2D coronal and 2D sagittal image which serve as the template images. These template images are then registered to a coronal and sagittal slice which is extracted from the 3D MRI dataset at the centroid location of the prostate. This registration can be manually edited by the user if necessary. In the next stage, live cine MRI images are automatically registered to the average 2D template images generated during the first stage (2D-2D). The total offset of the prostate in each cine frame is then equal to the summation of the initial 2D-3D registration plus the registration value of the 2D-2D matching. An example of the target tracking interface and live prostate identification by the MMRP algorithm is shown in Figure 1.

2.3 Online adaptive planning procedure incorporating target tracking

Both the standard PTV margin group and the reduced PTV margin group began with a standard adapt-to-shape workflow in the online environment (62). Briefly, a 2 min T2 weighted MRI image was acquired at the beginning of each treatment fraction. The prostate and OARs were contoured on each daily MRI dataset (50 fractions in total). Once contouring was completed a full optimization of the VMAT plans was performed using a pseudo gradient descent and optimal fluence levels optimizer within the research Monaco TPS (43). The standard margin plans were optimized with 1% statistical uncertainty per plan, 3 mm dose grid, and were scaled for 95% PTV coverage. Each reference plan was generated using two counterclockwise treatment fields with the first beam going from 179° to 21° and the second VMAT arc treating from 5° to 180°. This is equivalent to a single full VMAT arc, but without treating through the cryostat pipe of the MR linac (59). All plans used a minimum segment width of 0.75 cm and a maximum of 90 control points per beam. For the standard PTV margin group no further adaptation was performed and this group serves as a control for comparison with the intra-fraction re-optimization reduced PTV margin group as described below.

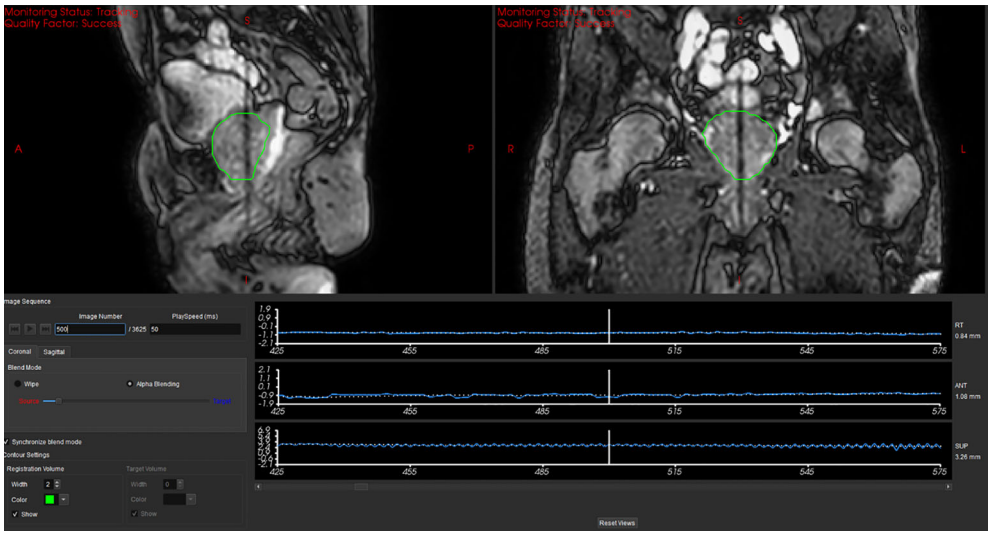

FIGURE 1
Screen Capture depicting the motion tracking software interface. The green contour represents the position of the prostate as identified by the tracking algorithm in the live cine MRI in a sagittal and coronal plane. The bottom of the image depicts the tracked position of the prostate in the right/left, ant/post, and sup/inf positions on the current frame as well as history of previous tracked positions.

For the reduced margin group, a novel workflow was performed which consisted of breaking the online treatment session into 4 sequential sub-fractions per treatment session. Each sub-fraction was planned to deliver a uniform 25% (1.8125 Gy) of the total treatment session dose. Essentially four subsequent VMAT arcs were used to deliver the total SBRT dose per fraction of 7.25 Gy. In this workflow, a re-optimization is performed in parallel with the delivery of each arc such that a new fully re-optimized plan that includes any intrafraction drift of the target is ready for delivery at the immediate conclusion of the current arc. Thus, intra-fraction adaptive plans will be delivered without any pauses in treatment delivery. Figure 2 shows a diagram depicting this workflow.

The aim of this workflow is to compensate for intra-fraction motion of the prostate and maintain prostate coverage with reduced PTV margins. To accomplish this goal, the position of the prostate, as identified by the tracking algorithm and cine MRI, would need to be synchronized with the radiation treatment delivery. Immediately after the original ATS optimization, an adapt-to-position (ATP) re-optimization technique would applied which shifts the MLC's based on the current position of the prostate and re-weights each IMRT segment to reproduce the dose distribution of the daily ATS plan (ATP "optimize weights") (62). This step would account for intra-fraction motion of the prostate which occurred during the re-contouring and original optimization timeframe. The first VMAT treatment arc would then be delivered following the ATP re-optimization. The Monaco treatment planning system reports the delivery time of each treatment beam and in this workflow a re-optimization would be triggered 65 seconds prior to the completion of the active VMAT arc. 65 seconds was chosen in this work and represents a conservative value to ensure that the plan would be finished optimizing and exporting prior to the completion of the active arc. Thus, the second arc begins delivery with a newly adapted sub-fraction plan which is corrected for intra-fraction motion. This process repeats until all four VMAT sub-fractions have been delivered. All plans using the reduced PTV margins were calculated with 2% statistical uncertainty per sub-fraction, 3 mm dose grid, and were scaled to 95% PTV coverage. The use of 2% statistical uncertainty speeds up optimization and because 4 repeated Monte Carlo calculations will be done, the final composite dose from all 4 fractions will have an inherent 1% statistical uncertainty per plan, which is commonly reported in clinical use. In addition, the use of 2% statistical uncertainty has been shown to have negligible dosimetric impact as compared to plans that use 1% statistical uncertainty per plan (63). The optimization and the reported delivery times for each sub-fraction were recorded. In total, an additional 200 intra-fractional adaptive plans were created in this study.

2.4 Sub-fraction workflow composite dose calculation and OAR comparison

Sub-fraction doses from each treatment session were rigidly registered back onto the daily MRI dataset. These sub-fraction doses were then summed to generate a composite daily fractional dose on the daily MRI dataset which was equal to 7.25 Gy per fraction, matching the standard margin dose and fractionation scheme. OAR doses from the composite reduced margin group were compared against the daily adapted ATS plans for the standard margin group. OAR dose metrics were evaluated at critical constraint values as specified by the PACE B trial (58). OAR metrics evaluated include V18 Gy, D1cc, D5cc for bladder and V18 Gy, and D1cc for the rectum. The tracking algorithm used in this study tracked the prostate only and is not capable of accounting for deformations like those commonly seen for the bladder and rectum. For these reasons, all reported OAR doses in this this study are as calculated

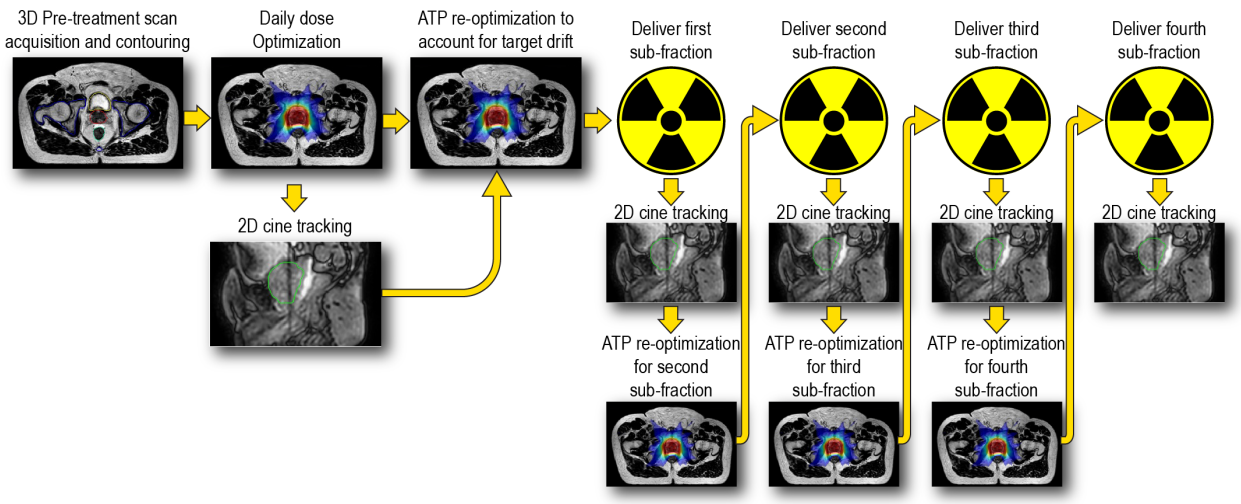

FIGURE 2
Overview of intra-fraction adaptive workflow incorporating near real time optimization in parallel with dose delivery. Cine MRI imaging starts at the onset of the intital dose optimizations and remains running throughout the entirety of the treatment session.

on the daily MRI dataset and do not account for intra-fractional motion. Differences between the standard and reduced PTV margin groups were evaluated for statistical significance for each individual DVH metric using a two sided t-test and 0.05 significance level.

2.5 Intra-fraction prostate motion and dose reconstruction

Sub-fraction doses were first rigidly registered onto the daily MRI dataset. Next, intra-fraction dose was accumulated following the methodology provided by Snyder et al. (39). Briefly, the prostate position as a function of time defined from the cine MRI images and target tracking was synchronized with the radiation therapy treatment delivery. The DICOM coordinates from each of the eight treatment arcs were shifted to account for the prostates average position during the delivery of that beam. In this scenario, the isocenter position of each beam was shifted to represent the effective motion of the beam with respect to the fixed reference of the prostate on the daily MRI image (39). The shifted beam doses were then summed and composite doses were viewed within Velocity (Varian Medical Systems Inc., Palo Alter, CA, version 3.2.1).

To evaluate the utility of the intra-fraction adaptive workflow, the motion trace from the cine MRI images were simulated under three scenarios, as depicted in Figure 3. In the first scenario, the motion trace was unaltered from the clinical delivery and thus represents no adaptation. This case reflects motion which occurs throughout the adaptive process time including contouring and ATS optimization. This is referred to as the "no-adapt" group. In the second scenario, the motion trace was modified to reflect performing an ATP virtual couch shift immediately prior to treatment. This strategy has been a previously reported workflow for MRIgART (29). In this scenario, no other intra-fraction corrections are considered and no further modifications were made to the prostate motion trace. This scenario is referred to as "ATP". The last scenario represents the full intra-fraction re-optimization technique proposed in this study. This scenario begins like the "ATP" group, but the prostate motion trace is further modified to reflect each time point when a new intra-fraction re-optimized plan were to begin. Therefore, this scenario includes four updates to the original prostate motion trace which correspond to time points at which the newly adapted plans begin. This scenario is referred to as "intra-adapt". Of note, the first 25% of the treatment session motion traces are the same for the "ATP" and "intra-adapt" groups.

The effect of intra-fraction motion on the dose received by the prostate was compared for each scenario. Coverage metrics include prostate V36.25 Gy, minimum dose received by the prostate, and PTV V36.25 Gy. Statistical significance was assessed using a one-way ANOVA and a Bonferroni *post hoc* analysis.

3 Results

3.1 OAR dosimetric comparison of reduced and standard PTV margins

All plans in this study meet the mandatory dosimetric constraints for prostate SBRT as defined by our institutional standards. This includes all reference plans, all ATS plans in the standard PTV margin group, and all the composite sub-fraction workflow adapted plans in the reduced margin group. The average separation between the prostate and rectum created by the SpaceOAR was 0.9 ± 0.4 cm (range 0.3 – 1.6 cm). The intra-fraction composite plans in the reduced margin group had statistically significant reductions in all DVH points analyzed in this study including bladder V18 Gy, D1cc, D5cc, and rectum V18 Gy and D1cc. Bladder DVH metrics were reduced by 7.8 ± 5.6% for V18 Gy ($p<0.001$), 9.6 ± 7.3% (3.4 ± 2.5 Gy) for D1cc ($p<0.001$),

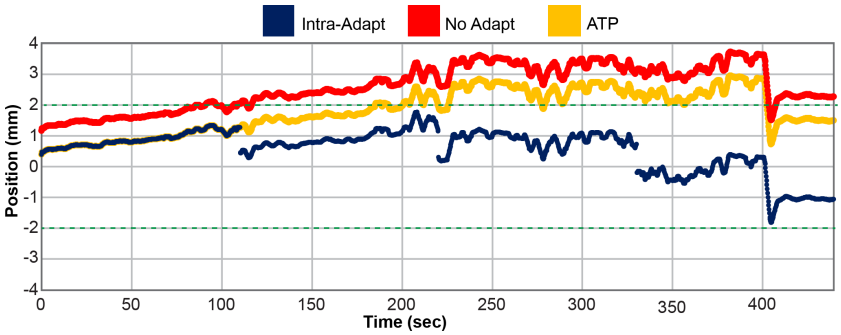

FIGURE 3
Prostate motion trace for patient 5 fraction number 4 in the Anterior (-) and Posterior (+) direction. The position of the prostate is plotted as a function of time for the unaltered no adapt motion trace (red), motion trace where adaption was only applied prior the start of treatment (ATP) (yellow), and for the full intra-fraction adaptive workflow (intra-adapt) (navy blue). The green dashed horizontal line depicts the uniform 2 mm PTV margin expansion from the originally planned prostate position.

and 21.9 ± 10.3% (6.9 ± 3.0 Gy) for D5cc ($p<0.001$). Rectum V18 Gy was reduced by 4.4 ± 3.9% ($p<0.001$) and D1cc was reduced by 12.2 ± 6.8% (3.4 ± 2.3 Gy) ($p<0.001$). All of these DVH metrics are based on OAR contours generated on the daily MRI datasets and do not account for intra-fraction motion. Per patient bladder DVH metrics are displayed in the box and whisker plot in Figure 4 and per patient rectum metrics are shown in Figure 5.

3.2 Intra-fraction re-optimization timing and prostate motion trace

The average time to complete intra-fraction re-optimizations among all 200 sub-fractions was 40.0 ± 2.9 seconds while the average time to deliver a single sub-fraction was estimated to be 104.4 ± 9.3 seconds. With this approach, every re-optimization would be completed prior to the completion of the sub-fraction currently being delivered. Thus, the proposed intra-fraction optimization workflow would not cause any interruptions in treatment delivery. The average per patient re-optimization times among all 20 fractions and sub-fraction delivery times are shown in Table 1.

Figure 3 shows an example of a single fraction motion trace for patient 5 in the anterior (–) and posterior (+) directions. The motion trace with no adaptions reaches an excursion of nearly 4 mm with respect to the originally planned prostate position, while the ATP group had a maximum excursion of 3 mm and the intra-adapt group had an excursion of less than 2 mm. This is a representative fraction from this study. The no-adapt motion trace does not start at 0 mm at time point zero because of prostate drift that occurred during the adaptive planning process. The Intra-adapt and ATP groups also do not start at time point zero because the adaptions do not instantaneously take effect. Optimization is initiated and during the re-planning process the prostate position can drift before the new sub-fraction is ready for delivery. Figure 3 highlights the benefits of using the intra-adaptive workflow to reduce prostate excursions from the planned position during treatment delivery.

Figure 6 shows the composite motion traces from all 50 fractions of the no-adapt (A-C), ATP (D-F), and intra-adapt (G-I) groups. The average position of the prostate among all fractions for each time point is depicted by the blue line and the standard deviation at each time point is shown by the yellow color wash. During planning and treatment delivery the average position of the prostate had a systematic drift in the inferior direction as noted by the negative values in Figure 6C and a small systematic drift in the posterior direction (Figure 6B). The standard deviation in the position of the target at the onset of treatment was greatest for the no adapt-group, attributed to the fact that the motion was not accounted for with an ATP plan directly prior to treatment. At the final time point in in Figure 6 (treatment completion), the magnitude and standard deviation of the prostate as compared to the initial planned position was -0.39 ± 1.72 mm (Left/Right), 0.09 ± 1.72 mm (Ant/Post), and -1.86 ± 2.82 mm (sup/inf) for the no-adapt group, 0.03 ± 0.44 mm (Left/Right), 0.17 ± 0.98 mm (Ant/Post), and -0.62 ± 1.68 mm (sup/inf) for the ATP group, and -0.02 ± 0.21 mm (Left/Right), 0.19 ± 0.46 mm (Ant/Post), and -0.33 ± 0.65 mm (sup/inf) for the intra-adapt group. This shows that the intra-adapt workflow effectively corrects the systematic prostate drift observed in the no-adapt group. The intra-adapt workflow also has the smallest variability in prostate position at the end of each treatment session delivery, as indicated by the intra-adapt group having the smallest standard deviation in each of the three principal motion directions.

3.3 Intra-fraction reconstructed prostate and PTV dose coverage

The delivered dose of the day was reconstructed while accounting for intra-fraction motion of the prostate. The percentage of the prostate covered by the prescription isodose line (V36.25 Gy) was on average 96.5 ± 4.0%, 99.1 ± 1.3%, and 99.6 ± 0.4 for the non-adapt, ATP, and intra-adapt groups, respectively. The minimum dose received by the prostate was on average 31.5 ± 4.7 Gy, 34.4 ± 1.7 Gy and 35.1 ± 0.8 Gy for the non-adapt, ATP, and

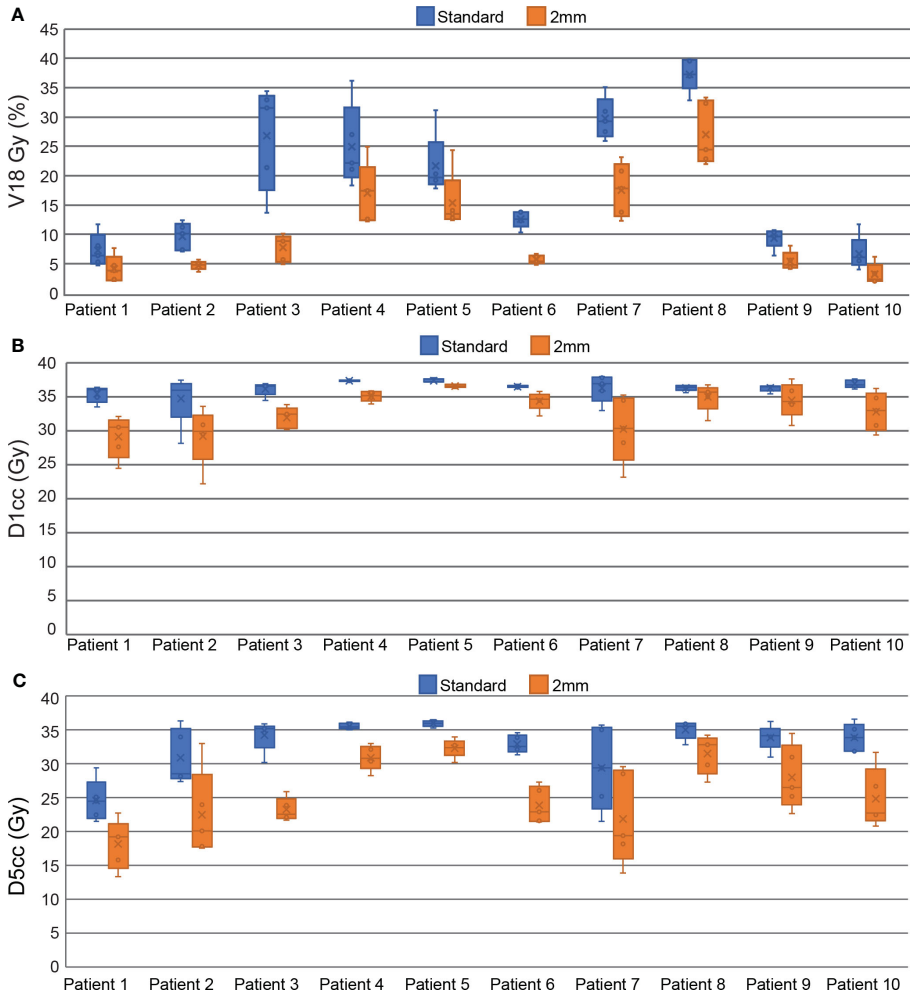

FIGURE 4
Box and Whisker plots comparing standard and reduced margin plans at key bladder dosimetric constraint values including V18 Gy **(A)**, D1cc **(B)**, and D5cc **(C)**.

intra-adapt groups, respectively. The minimum dose received by the prostate was less than 95% of the prescription dose in 84%, 36%, and 10% of fractions, for the non-adapt, ATP, and intra-adapt groups, respectively. The PTV V36.25 Gy was on average 90.0 ± 4.7%, 94.6 ± 2.4%, and 95.6 ± 1.2 for the non-adapt, ATP, and intra-adapt groups, respectively. For all metrics evaluated, the intra-adapt group had the smallest variability, thus having smaller deviations with respect to prescribed dose on the static daily MRI image.

Figure 7 displays the per patient intra-fraction accumulated DVH statistics for prostate V36.25 Gy (A), PTV V36.25 Gy (B), and the minimum dose received by the prostate (C). The box and whisker plot represents the statistics from each of the 5 fractions for each patient.

4 Discussions

Reducing margins in prostate radiotherapy remains a challenge due to intra-fraction motion. MRIgART can track targets without using invasive fiducial implants or additional ionizing radiation which is advantageous over tracking methodologies on conventional linear accelerators. However, the Elekta Unity MR linac design does not support couch motion (52) and therefore intra-fraction baseline shift corrections require a re-calculation and/or re-optimization. Reduced PTV margins will necessitate more frequent intra-fraction adaptions and re-optimizations. This may significantly decrease the beam-on duty cycle and add extra time to the treatment delivery. MRIgART already has a limitation of long treatment session times, therefore intra-fraction adaptive techniques which add extra treatment time are not desirable. This study overcomes that limitation by simulating the feasibility of an intra-fraction re-optimization workflow based on the position of the target extracted from the 2D cine images acquired during treatment delivery that can be performed in parallel with radiation delivery such that no beam pauses are required.

The commonly used Van Herk PTV margin methodology is designed to ensure that 90% of patients receive a minimum CTV dose of at least 95% of the prescription dose (64). In this study we

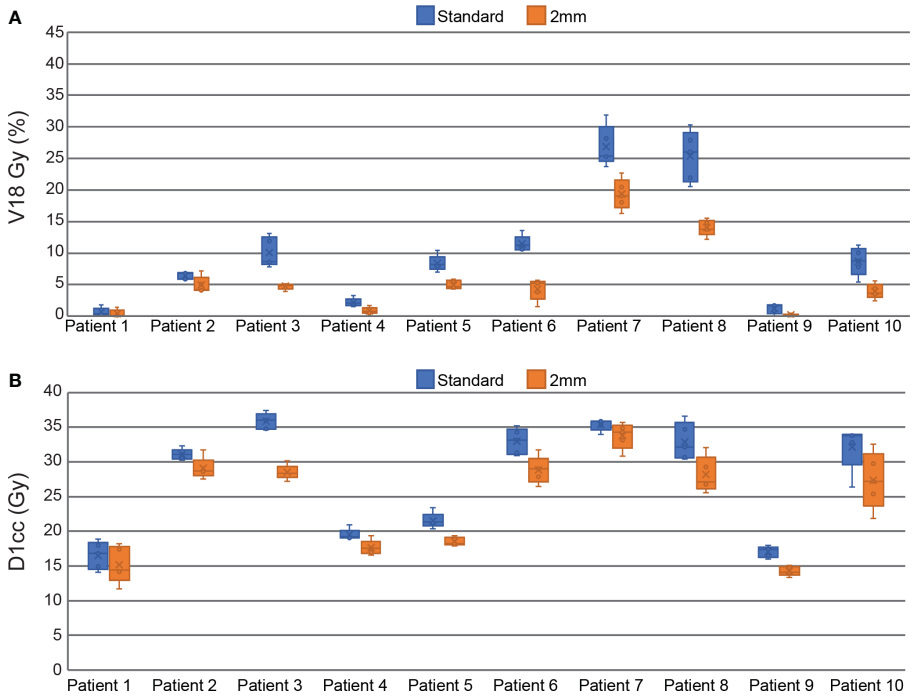

FIGURE 5
Box and Whisker plots comparing standard and reduced margin plans at key rectum dosimetric constraint values including V18 Gy **(A)**, and D1cc **(B)**.

found that this minimum dose metric was not met in 84%, 36%, and 10% of fractions when using the no-adapt, ATP, and intra-adapt methodologies with a 2 mm margin. Thus, our study has shown that 2 mm margins are not feasible for the no-adapt and ATP methodologies. This is similar to findings presented by Keizer et al. who reported that PTV margin reductions below 4 mm would require intra-fraction adaptions for prostate MRIgART treatments (29). Previously reported MRIgART motion management studies have focused on step-and-shoot IMRT deliveries while this study simulated a VMAT delivery technique. Willigenburg et al. reported prostate step-and-shoot delivery times of 11.0 minutes (65) while this study had an average total treatment session delivery time of 7.0 minutes. Despite the shorter treatment times afforded by VMAT, 2 mm margins were still not feasible without further intra-fraction corrections. However, by using the intra-adapt workflow, 2 mm PTV margins are feasible based on the Van Herk definition. While the intra-adapt workflow does add additional complexity, the ability to reduce PTV margins highlights its utility.

PTV margin reductions have been previously shown to provide superior OAR sparing in prostate SBRT (23). This study found statistically significant reductions for all DVH metrics in the reduced margin group as compared to the standard PTV margin group. This will likely lead to decreased GU and GI toxicities as demonstrated by the MIRAGE trial (18). Improved OAR sparing may be even more critical in studies which attempt to perform even

TABLE 1 Intra-fraction workflow timing.

	Intra-fraction optimization time (sec)	Estimated sub-fraction delivery time (sec)	total treatment delivery time (sec)
Patient 1	41.8 ± 2.7	111.6 ± 17.0	446.3 ± 68.0
Patient 2	41.6 ± 2.8	108.4 ± 5.1	433.5 ± 20.6
Patient 3	39.7 ± 1.7	104.4 ± 4.4	417.6 ± 17.6
Patient 4	37.9 ± 1.8	104.0 ± 4.5	416.0 ± 18.1
Patient 5	40.0 ± 1.3	102.3 0± 4.6	409.2 ± 18.3
Patient 6	35.3 ± 2.4	110.6 0± 11.1	442.3 ± 44.4
Patient 7	40.0 ± 1.8	95.3 0± 3.9	381.4 ± 15.7
Patient 8	42.1 ± 1.4	93.7 0± 2.8	374.6 ± 11.2
Patient 9	43.2 ± 1.2	101.1 0± 3.5	404.4 ± 14.0
Patient 10	38.9 ± 1.3	113.1 0± 6.2	452.6 ± 24.9

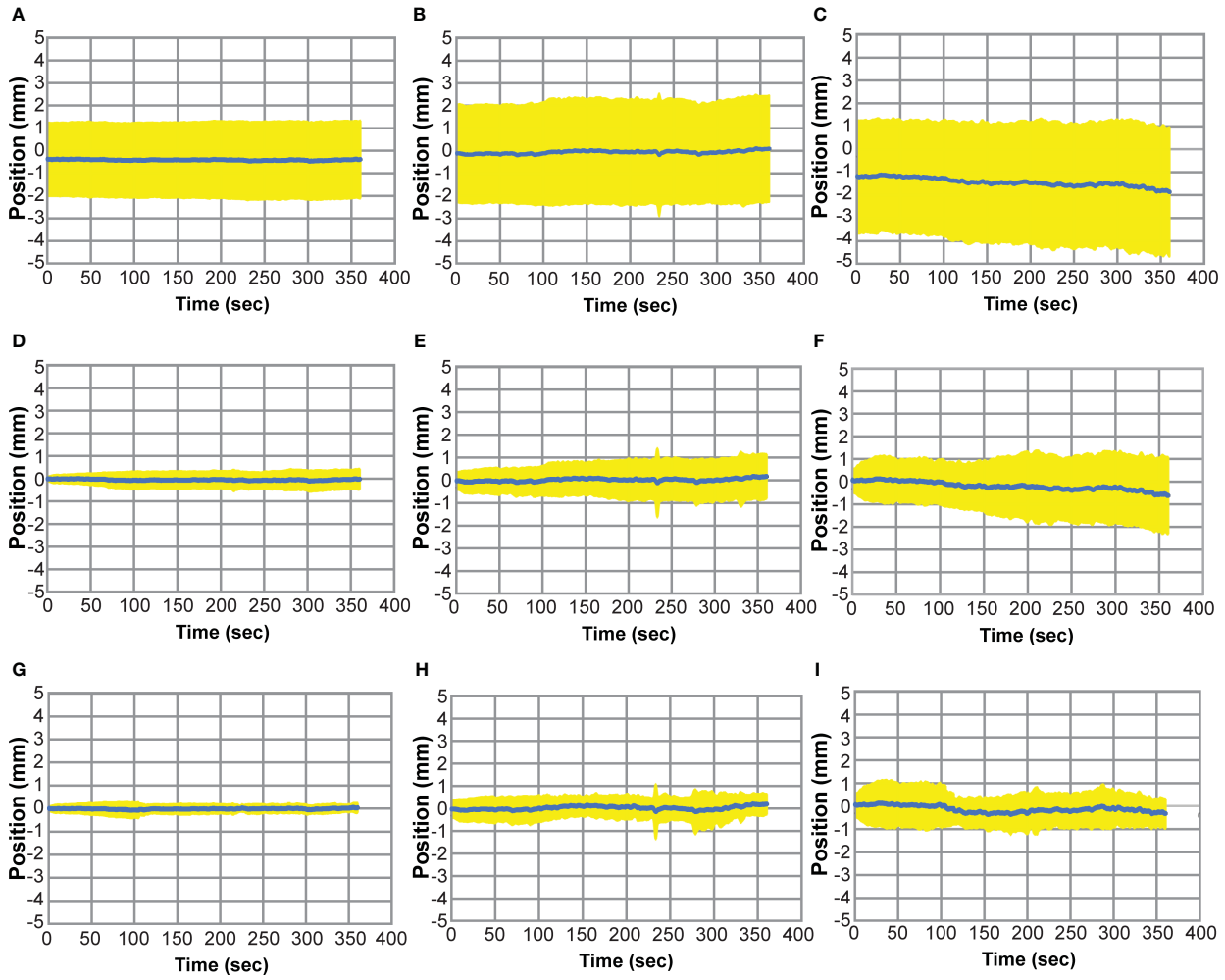

FIGURE 6
Prostate Motion Traces where the average prostate position (blue) is shown as a function of time over all treatment fractions and the standard deviation at each time point is shown in yellow. Motion traces for the non-adapt group are shown for left (+)/right (-) **(A)**, ant (-)/post (+) **(B)**, and sup (+)/inf (-) **(C)**. Motion traces for the ATP group are shown for left/right **(D)**, sup/inf **(E)**, and ant/post **(F)**. Motion traces for the intra-adapt group are shown for left/right **(G)**, sup/inf **(H)**, and ant/post **(I)**.

more extreme hypofractionation and treat the prostate in one to two fractional doses (66, 67). Reducing margins to better spare OARs is also of paramount importance in SBRT re-irradiation in the recurrent prostate setting (68).

Prior studies have shown that intra-fraction motion can degrade OAR sparing in MRIgRT by comparing pre and post image MRI scans. Brennan et al. found that urethral sparing was achieved in 92% of fractions as defined in the pre MRI scan but that number degraded to 66% of fractions meeting the same dosimetric constraint on the post MRI image (69). Similarly Dang et al. found that intra-fraction motion caused a statistically significant increase in the bladder D5cc dose (70). While the primary focus of this study was to reconstruct the daily delivered dose to the prostate, it is our hypothesis that the proposed intra-fraction re-planning workflow will also reduce the degradation in OAR sparing caused by intra-fraction motion. Future studies should be designed to test this which use intra-fraction imaging to specifically track these OARs and which are capable of tracking non-rigid structures.

Recently, a sub-fraction workflow in MRIgART was proposed by Willigenburg et al. (65). In this study, a 3D MRI image was acquired in parallel with IMRT treatment delivery and an ATP adaptation was performed based on the target position on the intra-fraction 3D MRI scan while the first half of treatment was being delivered. The novelty of our work comes from the increased efficiency of using cine MRI imaging to perform multiple re-optimizations within one treatment session while allowing continuous live tracking of the prostate such that the beam can be paused should any large sudden motions occur. The proposed workflow incorporates VMAT and enables uninterrupted treatment from arc to arc. In this work sub-fractions took on average 94.5 seconds to deliver while optimization was performed in 40.1 seconds on average. This differential highlights that an even larger number of sub-fractions could be implemented for patients who experience consistently large intrafraction motion without causing treatment pauses while waiting for the new treatment plan.

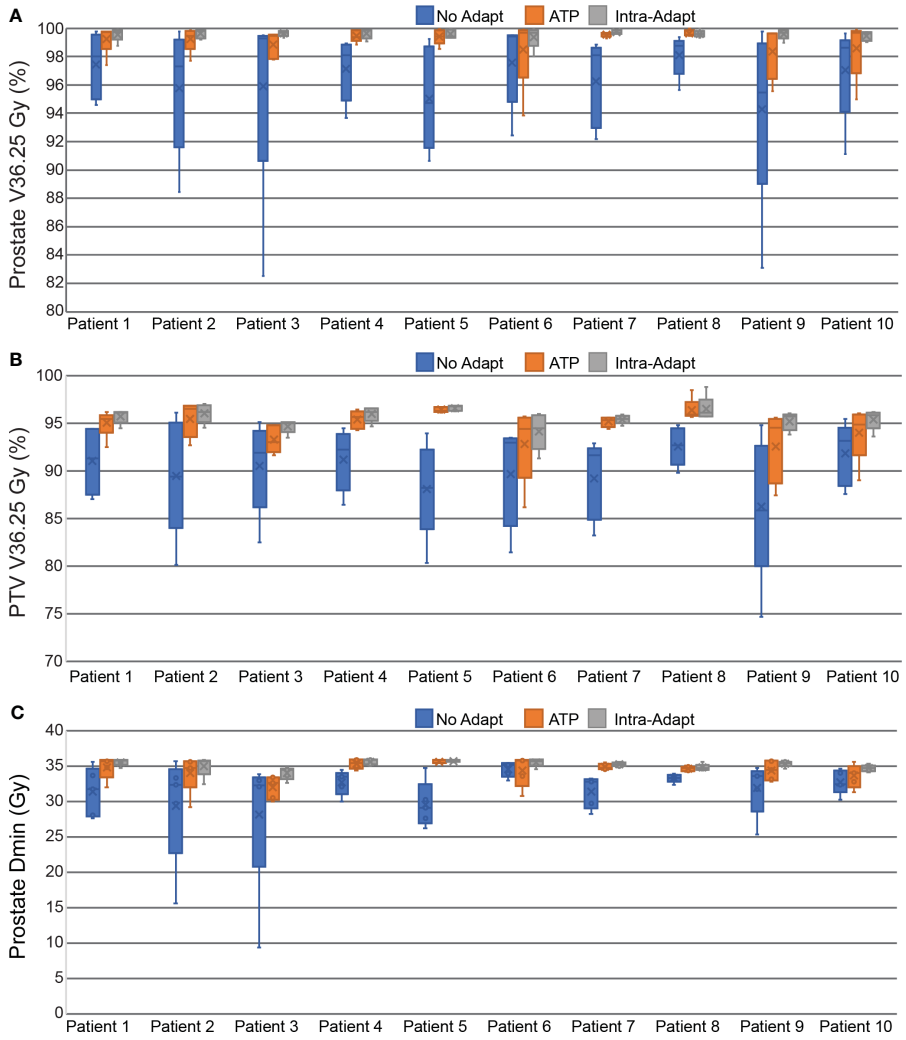

FIGURE 7
Box and Whisker plots measuring the dosimetric impact of prostate intra-fraction motion during treatment delivery. Dose and coverage statistics are shown for the prostate V36.25 Gy **(A)**, PTV V36.25 Gy **(B)**, and the minimum dose received by the prostate **(C)**.

The ability to efficiently perform multiple sub-fraction adaptations showed the feasibility of using 2 mm margins while Wiligenburg's sub-fraction workflow, while beneficial, still required PTV margins up to 2.6 mm. Since each VMAT arc delivers a uniform 25% of the treatment session dose, no intra-fraction deformable dose accumulation was needed. This is a similar strategy to that employed by Willigneburg (65) and simplifies the online re-optimization.

While this work focused on using SBRT to treat the entire prostate it can also be extended to simultaneous integrated boost techniques in cases where the GTV is identifiable. Currently, the balanced cine MRI imaging sequence would not provide adequate contrast to track the GTV directly, but this intrafraction sub-fraction workflow could be employed if the prostate and GTV are assumed to move as a rigid body throughout the course of each fraction. Cine MRI imaging sequences with different weightings may enable direct tracking of the gross tumor within the prostate in the future.

One of the limitations of this study is the relatively small number of patients evaluated. However, this study was able to achieve statistically significant differences in OAR sparing and target coverage between each adaptive strategy and PTV margin group. While the number of patients was small, a total of 320 plans were evaluated between reference and adaptive plans.

5 Conclusion

When using reduced PTV margins, intra-fraction adaptation is needed to account for prostate motion and to prevent underdosage to the prostate and PTV. Reduced PTV margins provide superior OAR sparing as compared to standard margin expansions. The intra-fraction workflow described in this study provides a novel methodology to counteract prostate intra-fraction motion without reducing treatment duty cycle and while allowing continuous CINE imaging for motion monitoring. Uniform 2 mm PTV margins are

feasible with the described intra-fraction VMAT arc re-optimization strategy.

Data availability statement

The datasets presented in this article are not readily available because the anonymized datasets used for this research are not currently available for public use. Requests to access the datasets should be directed to jeffrey-snyder@uiowa.edu.

Ethics statement

The studies involving humans were approved by University of Iowa Institutional Review Board. The studies were conducted in accordance with the local legislation and institutional requirements. The participants provided their written informed consent to participate in this study.

Author contributions

JS: Conceptualization, Data curation, Formal analysis, Funding acquisition, Investigation, Methodology, Validation, Visualization, Writing – original draft. BS: Software, Writing – review & editing. JSA: Writing – review & editing. AS: Writing – review & editing. DH: Conceptualization, Funding acquisition, Supervision, Writing – review & editing.

Funding

The author(s) declare financial support was received for the research, authorship, and/or publication of this article. This work was partially supported through a research grant with Elekta AB, Stockholm Sweden.

Conflict of interest

DH has received consulting fees, and travel support from Elekta AB for work not related to this study. JS and JSA have received Honoria and travel support from Eletka AB which is not related to this work.

The remaining authors declare that the research was conducted in the absence of any commercial or financial relationships that could be constructed as a potential conflict of interest.

Publisher's note

All claims expressed in this article are solely those of the authors and do not necessarily represent those of their affiliated organizations, or those of the publisher, the editors and the reviewers. Any product that may be evaluated in this article, or claim that may be made by its manufacturer, is not guaranteed or endorsed by the publisher.

References

1. *Key Statistics for Prostate Cancer: American Cancer Society* (2023). Available at: https://www.cancer.org/cancer/types/prostate-cancer/about/key-statistics.html.

2. Barton MB, Jacob S, Shafiq J, Wong K, Thompson SR, Hanna TP, et al. Estimating the demand for radiotherapy from the evidence: a review of changes from 2003 to 2012. *Radiotherapy Oncol* (2014) 112(1):140–4. doi: 10.1016/j.radonc.2014.03.024

3. Delaney G, Jacob S, Barton M. Estimating the optimal external-beam radiotherapy utilization rate for genitourinary Malignancies. *Cancer* (2005) 103 (3):462–73. doi: 10.1002/cncr.20789

4. Rebello RJ, Oing C, Knudsen KE, Loeb S, Johnson DC, Reiter RE, et al. Prostate cancer. *Nat Rev Dis primers.* (2021) 7(1):9. doi: 10.1038/s41572-020-00243-0

5. Miralbell R, Roberts SA, Zubizarreta E, Hendry JH. Dose-fractionation sensitivity of prostate cancer deduced from radiotherapy outcomes of 5,969 patients in seven international institutional datasets: α/β = 1.4 (0.9–2.2) Gy. *Int J Radiat OncologyBiologyPhysics* (2012) 82(1):e17–24. doi: 10.1016/j.ijrobp.2010.10.075

6. Vogelius IR, Bentzen SM. Meta-analysis of the alpha/beta ratio for prostate cancer in the presence of an overall time factor: bad news, good news, or no news? *Int J Radiat oncology biology Phys* (2013) 85(1):89–94. doi: 10.1016/j.ijrobp.2012.03.004

7. Brenner DJ, Hall EJ. Fractionation and protraction for radiotherapy of prostate carcinoma. *Int J Radiat oncology biology physics.* (1999) 43(5):1095–101. doi: 10.1016/S0360-3016(98)00438-6

8. Dasu A, Toma-Dasu I. Prostate alpha/beta revisited – an analysis of clinical results from 14 168 patients. *Acta Oncologica.* (2012) 51(8):963–74. doi: 10.3109/0284186X.2012.719635

9. Di Franco R, Borzillo V, Ravo V, Ametrano G, Falivene S, Cammarota F, et al. Rectal/urinary toxicity after hypofractionated vs conventional radiotherapy in low/intermediate risk localized prostate cancer: systematic review and meta analysis. *Oncotarget* (2017) 8(10):17383–95. doi: 10.18632/oncotarget.14798

10. Malouff TD, Stross WC, Seneviratne DS, Waddle MR, May BC, Buskirk SJ, et al. Current use of stereotactic body radiation therapy for low and intermediate risk prostate cancer: A National Cancer Database Analysis. *Prostate Cancer prostatic diseases.* (2020) 23(2):349–55. doi: 10.1038/s41391-019-0191-9

11. Tree AC, Ostler P, van der Voet H, Chu W, Loblaw A, Ford D, et al. Intensity-modulated radiotherapy versus stereotactic body radiotherapy for prostate cancer (PACE-B): 2-year toxicity results from an open-label, randomised, phase 3, non-inferiority trial. *Lancet Oncol* (2022) 23(10):1308–20. doi: 10.1016/S1470-2045(22)00517-4

12. Widmark A, Gunnlaugsson A, Beckman L, Thellenberg-Karlsson C, Hoyer M, Lagerlund M, et al. Ultra-hypofractionated versus conventionally fractionated radiotherapy for prostate cancer: 5-year outcomes of the HYPO-RT-PC randomised, non-inferiority, phase 3 trial. *Lancet (London England).* (2019) 394(10196):385–95. doi: 10.1016/S0140-6736(19)31131-6

13. Incrocci L, Wortel RC, Alemayehu WG, Aluwini S, Schimmel E, Krol S, et al. Hypofractionated versus conventionally fractionated radiotherapy for patients with localised prostate cancer (HYPRO): final efficacy results from a randomised, multicentre, open-label, phase 3 trial. *Lancet Oncol* (2016) 17(8):1061–9. doi: 10.1016/S1470-2045(16)30070-5

14. Benedict SH, Yenice KM, Followill D, Galvin JM, Hinson W, Kavanagh B, et al. Stereotactic body radiation therapy: The report of AAPM Task Group 101. *Med Physics.* (2010) 37(8):4078–101. doi: 10.1118/1.3438081

15. Hodges JC, Lotan Y, Boike TP, Benton R, Barrier A, Timmerman RD. Cost-effectiveness analysis of stereotactic body radiation therapy versus intensity-modulated radiation therapy: an emerging initial radiation treatment option for organ-confined prostate cancer. *J Oncol Pract* (2012) 8(3 Suppl):e31s–7s. doi: 10.1200/JOP.2012.000548

16. Pan HY, Jiang J, Hoffman KE, Tang C, Choi SL, Nguyen Q-N, et al. Comparative toxicities and cost of intensity-modulated radiotherapy, proton radiation, and stereotactic body radiotherapy among younger men with prostate cancer. *J Clin Oncol* (2018) 36(18):1823–30. doi: 10.1200/JCO.2017.75.5371

17. Alongi F, Cozzi L, Arcangeli S, Iftode C, Comito T, Villa E, et al. Linac based SBRT for prostate cancer in 5 fractions with VMAT and flattening filter free beams:

preliminary report of a phase II study. *Radiat Oncol* (2013) 8(1):171. doi: 10.1186/1748-717X-8-171

18. Kishan AU, Lamb J, Casado M, Wang X, Ma TM, Low D, et al. Magnetic resonance imaging-guided versus computed tomography-guided stereotactic body radiotherapy for prostate cancer (MIRAGE): Interim analysis of a phase III randomized trial. *J Clin Oncol* (2022) 40(6_suppl):255. doi: 10.1200/JCO.2022.40.6_suppl.255

19. Sandler HM, Liu PY, Dunn RL, Khan DC, Tropper SE, Sanda MG, et al. Reduction in patient-reported acute morbidity in prostate cancer patients treated with 81-Gy Intensity-modulated radiotherapy using reduced planning target volume margins and electromagnetic tracking: assessing the impact of margin reduction study. *Urology* (2010) 75(5):1004–8. doi: 10.1016/j.urology.2009.10.072

20. van Herk M, Bruce A, Guus Kroes AP, Shouman T, Touw A, Lebesque JV. Quantification of organ motion during conformal radiotherapy of the prostate by three dimensional image registration. *Int J Radiat OncologyBiologyPhysics.* (1995) 33 (5):1311–20. doi: 10.1016/0360-3016(95)00116-6

21. Xie Y, Djajaputra D, King CR, Hossain S, Ma L, Xing L. Intrafractional motion of the prostate during hypofractionated radiotherapy. *Int J Radiat oncology biology physics.* (2008) 72(1):236–46. doi: 10.1016/j.ijrobp.2008.04.051

22. Shintani T, Anami S, Sano K, Okada W, Tanooka M. Stereotactic body radiation therapy for prostate cancer using tomotherapy with synchrony fiducial tracking. *Cureus* (2023) 15(6):e40778. doi: 10.7759/cureus.40778

23. Gill SK, Reddy K, Campbell N, Chen C, Pearson D. Determination of optimal PTV margin for patients receiving CBCT-guided prostate IMRT: comparative analysis based on CBCT dose calculation with four different margins. *J Appl Clin Med Phys* (2015) 16(6):252–62. doi: 10.1120/jacmp.v16i6.5691

24. Bright M, Foster RD, Robinson M, Ruiz JL, Hampton CJ, Moeller BJ, et al. Dosimetric effects of intrafraction motion detected by triggered imaging during prostate SBRT. *Int J Radiat OncologyBiologyPhysics* (2019) 105(1, Supplement):E748. doi: 10.1016/j.ijrobp.2019.06.862

25. Yartsev S, Bauman G. Target margins in radiotherapy of prostate cancer. *Br J Radiol* (2016) 89(1067):20160312. doi: 10.1259/bjr.20160312

26. Tanaka S, Kadoya N, Ishizawa M, Katsuta Y, Arai K, Takahashi H, et al. Evaluation of Unity 1.5 T MR-linac plan quality in patients with prostate cancer. *J Appl Clin Med Phys* (2023) n/a(n/a):e14122. doi: 10.1002/acm2.14122

27. de Muinck Keizer DM, Kerkmeijer LGW, Willigenburg T, van Lier ALHMW, Hartogh M, van der Voort van Zyp JRN, et al. Prostate intrafraction motion during the preparation and delivery of MR-guided radiotherapy sessions on a 1.5T MR-Linac. *Radiotherapy Oncol* (2020) 151:88–94. doi: 10.1016/j.radonc.2020.06.044

28. Draulans C, van der Heide UA, Haustermans K, Pos FJ, van der Voort van Zyp J, De Boer H, et al. Primary endpoint analysis of the multicentre phase II hypo-FLAME trial for intermediate and high risk prostate cancer. *Radiotherapy Oncol* (2020) 147:92–8. doi: 10.1016/j.radonc.2020.03.015

29. de Muinck Keizer DM, van der Voort van Zyp JRN, de Groot-van Breugel EN, Raaymakers BW, Lagendijk JJW, de Boer HCJ. On-line daily plan optimization combined with a virtual couch shift procedure to address intrafraction motion in prostate magnetic resonance guided radiotherapy. *Phys Imaging Radiat Oncol* (2021) 19:90–5. doi: 10.1016/j.phro.2021.07.010

30. Chaurasia AR, Sun KJ, Premo C, Brand T, Tinnel B, Barczak S, et al. Evaluating the potential benefit of reduced planning target volume margins for low and intermediate risk patients with prostate cancer using real-time electromagnetic tracking. *Adv Radiat Oncol* (2018) 3(4):630–8. doi: 10.1016/j.adro.2018.06.004

31. Vanhanen A, Poulsen P, Kapanen M. Dosimetric effect of intrafraction motion and different localization strategies in prostate SBRT. *Physica Medica.* (2020) 75:58–68. doi: 10.1016/j.ejmp.2020.06.010

32. Mangesius J, Seppi T, Ibrahim R, Fleischmann K, Ginestet A, Vorbach S, et al. Dynamic intrafractional position monitoring with implanted fiducial markers for enhanced accuracy in radiotherapy of prostate cancer. *Phys Eng Sci Med* (2023) 46 (4):1365–74. doi: 10.1007/s13246-023-01304-w

33. Kaur G, Lehmann J, Greer P, Simpson J. Assessment of the accuracy of truebeam intrafraction motion review (IMR) system for prostate treatment guidance. *Australas Phys Eng Sci Med* (2019) 42(2):585–98. doi: 10.1007/s13246-019-00760-7

34. Bertholet J, Knopf A, Eiben B, McClelland J, Grimwood A, Harris E, et al. Real-time intrafraction motion monitoring in external beam radiotherapy. *Phys Med Biol* (2019) 64(15):15TR01–1. doi: 10.1088/1361-6560/ab2ba8

35. O'Shea T, Bamber J, Fontanarosa D, van der Meer S, Verhaegen F, Harris E. Review of ultrasound image guidance in external beam radiotherapy part II: intra-fraction motion management and novel applications. *Phys Med Biol* (2016) 61(8):R90. doi: 10.1088/0031-9155/61/8/R90

36. Gorovets D, Burleson S, Jacobs L, Ravindranath B, Tierney K, Kollmeier M, et al. Prostate SBRT with intrafraction motion management using a novel linear accelerator–based MV-kV imaging method. *Pract Radiat Oncol* (2020) 10(5):e388–e96. doi: 10.1016/j.prro.2020.04.013

37. Kisivan K, Antal G, Gulyban A, Glavak C, Laszlo Z, Kalincsak J, et al. Triggered imaging with auto beam hold and pre-/posttreatment CBCT during prostate SABR: analysis of time efficiency, target coverage, and normal volume changes. *Pract Radiat Oncol* (2021) 11 (2):e210–e8. doi: 10.1016/j.prro.2020.04.014

38. Xiong Y, Rabe M, Nierer L, Kawula M, Corradini S, Belka C, et al. Assessment of intrafractional prostate motion and its dosimetric impact in MRI-guided online adaptive radiotherapy with gating. *Strahlentherapie und Onkologie: Organ der Deutschen Rontgengesellschaft [et al].* (2023) 199(6):544–53. doi: 10.1007/s00066-022-02005-1

39. Snyder J, Smith B, St-Aubin J, Dunkerley D, Shepard A, Caster J, et al. Intra-fraction motion of pelvic oligometastases and feasibility of PTV margin reduction using MRI guided adaptive radiotherapy. *Front Oncol* (2023) 13. doi: 10.3389/fonc.2023.1098593

40. Peng C, Ahunbay E, Chen G, Anderson S, Lawton C, Li XA. Characterizing interfraction variations and their dosimetric effects in prostate cancer radiotherapy. *Int J Radiat OncologyBiologyPhysics.* (2011) 79(3):909–14. doi: 10.1016/j.ijrobp.2010.05.008

41. Leeman JE, Shin K-Y, Chen Y-H, Mak RH, Nguyen PL, D'Amico AV, et al. Acute toxicity comparison of magnetic resonance-guided adaptive versus fiducial or computed tomography-guided non-adaptive prostate stereotactic body radiotherapy: A systematic review and meta-analysis. *Cancer* (2023) 129(19):3044–52. doi: 10.1002/cncr.34836

42. Wahlstedt I, Andratschke N, Behrens CP, Ehrbar S, Gabryś HS, Schüler HG, et al. Gating has a negligible impact on dose delivered in MRI-guided online adaptive radiotherapy of prostate cancer. *Radiotherapy Oncol* (2022) 170:205–12. doi: 10.1016/j.radonc.2022.03.013

43. Snyder JE, St-Aubin J, Yaddanapudi S, Marshall S, Strand S, Kruger S, et al. Reducing MRI-guided radiotherapy planning and delivery times via efficient leaf sequencing and segment shape optimization algorithms. *Phys Med Biol* (2022) 67. doi: 10.1088/1361-6560/ac5299

44. Tetar SU, Bruynzeel AME, Lagerwaard FJ, Slotman BJ, Bohoudi O, Palacios MA. Clinical implementation of magnetic resonance imaging guided adaptive radiotherapy for localized prostate cancer. *Phys Imaging Radiat Oncol* (2019) 9:69–76. doi: 10.1016/j.phro.2019.02.002

45. Sandoval ML, Youssef I, Latifi K, Grass GD, Torres-Roca J, Rosenberg S, et al. Non-adaptive MR-guided radiotherapy for prostate SBRT: less time, equal results. *J Clin Med* (2021) 10(15):3396. doi: 10.3390/jcm10153396

46. Ristau J, Hörner-Rieber J, Buchele C, Klüter S, Jäkel C, Baumann L, et al. Stereotactic MRI-guided radiation therapy for localized prostate cancer (SMILE): a prospective, multicentric phase-II-trial. *Radiat Oncol* (2022) 17(1):75. doi: 10.1186/s13014-022-02047-w

47. Willigenburg T, van der Velden JM, Zachiu C, Teunissen FR, Lagendijk JJW, Raaymakers BW, et al. Accumulated bladder wall dose is correlated with patient-reported acute urinary toxicity in prostate cancer patients treated with stereotactic, daily adaptive MR-guided radiotherapy. *Radiotherapy Oncol* (2022) 171:182–8. doi: 10.1016/j.radonc.2022.04.022

48. Menten MJ, Mohajer JK, Nilawar R, Bertholet J, Dunlop A, Pathmanathan AU, et al. Automatic reconstruction of the delivered dose of the day using MR-linac treatment log files and online MR imaging. *Radiotherapy Oncol* (2020) 145:88–94. doi: 10.1016/j.radonc.2019.12.010

49. Alongi F, Rigo M, Figlia V, Cuccia F, Giaj-Levra N, Nicosia L, et al. Rectal spacer hydrogel in 1.5T MR-guided and daily adapted SBRT for prostate cancer: dosimetric analysis and preliminary patient-reported outcomes. *Br J Radiol* (2020) 94 (1117):20200848. doi: 10.1259/bjr.20200848

50. Schaule J, Chamberlain M, Wilke L, Baumgartl M, Krayenbühl J, Zamburlini M, et al. Intrafractional stability of MR-guided online adaptive SBRT for prostate cancer. *Radiat Oncol* (2021) 16(1):189. doi: 10.1186/s13014-021-01916-0

51. Alongi F, Rigo M, Figlia V, Cuccia F, Giaj-Levra N, Nicosia L, et al. 1.5 T MR-guided and daily adapted SBRT for prostate cancer: feasibility, preliminary clinical tolerability, quality of life and patient-reported outcomes during treatment. *Radiat Oncol* (2020) 15(1):69. doi: 10.1186/s13014-020-01510-w

52. Snyder JE, St-Aubin J, Yaddanapudi S, Boczkowski A, Dunkerley DAP, Graves SA, et al. Commissioning of a 1.5T Elekta Unity MR-linac: A single institution experience. *J Appl Clin Med Phys* (2020) 21(7):160–72. doi: 10.1002/acm2.12902

53. Raaymakers BW, Jürgenliemk-Schulz IM, Bol GH, Glitzner M, Kotte ANTJ, van Asselen B, et al. First patients treated with a 1.5 T MRI-Linac: clinical proof of concept of a high-precision, high-field MRI guided radiotherapy treatment. *Phys Med Biol* (2017) 62(23):L41–50. doi: 10.1088/1361-6560/aa9517

54. Muinck Keizer D, Willigenburg T, der Voort van Zyp J, Raaymakers BW, Lagendijk JJW, Boer J. Seminal vesicle intrafraction motion during the delivery of radiotherapy sessions on a 1.5 T MR-Linac. *Radiotherapy Oncol* (2021) 162:162–9. doi: 10.1016/j.radonc.2021.07.014

55. Uijtewaal P, Borman PTS, Woodhead PL, Kontaxis C, Hackett SL, Verhoeff J, et al. First experimental demonstration of VMAT combined with MLC tracking for single and multi fraction lung SBRT on an MR-linac. *Radiotherapy Oncol* (2022) 174:149–57. doi: 10.1016/j.radonc.2022.07.004

56. Kontaxis C, Woodhead PL, Bol GH, Lagendijk JJW, Raaymakers BW. Proof-of-concept delivery of intensity modulated arc therapy on the Elekta Unity 1.5 T MR-linac. *Phys Med Biol* (2021) 66(4):04LT1. doi: 10.1088/1361-6560/abd66d

57. Payne HA, Pinkawa M, Peedell C, Bhattacharyya SK, Woodward E, Miller LE. SpaceOAR hydrogel spacer injection prior to stereotactic body radiation therapy for men with localized prostate cancer: A systematic review. *Medicine* (2021) 100(49): e28111. doi: 10.1097/MD.0000000000028111

58. Brand DH, Tree AC, Ostler P, van der Voet H, Loblaw A, Chu W, et al. Intensity-modulated fractionated radiotherapy versus stereotactic body radiotherapy for prostate cancer (PACE-B): acute toxicity findings from an international, randomised, open-

label, phase 3, non-inferiority trial. *Lancet Oncol* (2019) 20(11):1531–43. doi: 10.1016/S1470-2045(19)30569-8

59. Dunkerley DAP, Hyer DE, Snyder JE, St-Aubin JJ, Anderson CM, Caster JM, et al. Clinical implementational and site-specific workflows for a 1.5T MR-linac. *J Clin Med* (2022) 11(6):1662. doi: 10.3390/jcm11061662

60. Jassar H, Tai A, Chen X, Keiper TD, Paulson E, Lathuilière F, et al. Real-time motion monitoring using orthogonal cine MRI during MR-guided adaptive radiation therapy for abdominal tumors on 1.5T MR-Linac. *Med Phys* (2023) 50(5):3103–16. doi: 10.1002/mp.16342

61. Keiper TD, Tai A, Chen X, Paulson E, Lathuilière F, Bériault S, et al. Feasibility of real-time motion tracking using cine MRI during MR-guided radiation therapy for abdominal targets. *Med Physics.* (2020) 47(8):3554–66. doi: 10.1002/mp.14230

62. Winkel D, Bol GH, Kroon PS, van Asselen B, Hackett SS, Werensteijn-Honingh AM, et al. Adaptive radiotherapy: The Elekta Unity MR-linac concept. *Clin Trans Radiat Oncol* (2019) 18. doi: 10.1016/j.ctro.2019.04.001

63. Rembish J, Myers P, Saenz D, Kirby N, Papanikolaou N, Stathakis S. Effects of varying statistical uncertainty using a Monte Carlo based treatment planning system for VMAT. *J BUON* (2021) 26(4):1683.

64. van Herk M. Errors and margins in radiotherapy. *Semin Radiat Oncol* (2004) 14 (1):52–64. doi: 10.1053/j.semradonc.2003.10.003

65. Willigenburg T, Zachiu C, Bol GH, de Groot-van Beugel EN, Lagendijk JJW, van der Voort van Zyp JRN, et al. Clinical application of a sub-fractionation workflow for intrafraction re-planning during prostate radiotherapy treatment on a 1.5 Tesla MR-Linac: A practical method to mitigate intrafraction motion. *Radiotherapy Oncol* (2022) 176:25–30. doi: 10.1016/j.radonc.2022.09.004

66. Alayed Y, Cheung P, Chu W, Chung H, Davidson M, Ravi A, et al. Two StereoTactic ablative radiotherapy treatments for localized prostate cancer (2STAR): Results from a prospective clinical trial. *Radiotherapy Oncol* (2019) 135:86–90. doi: 10.1016/j.radonc.2019.03.002

67. Zilli T, Scorsetti M, Zwahlen D, Franzese C, Förster R, Giaj-Levra N, et al. ONE SHOT - single shot radiotherapy for localized prostate cancer: study protocol of a single arm, multicenter phase I/II trial. *Radiat Oncol* (2018) 13(1):166. doi: 10.1186/s13014-018-1112-0

68. Baty M, Pasquier D, Gnep K, Castelli J, Delaby N, Lacornerie T, et al. Achievable dosimetric constraints in stereotactic reirradiation for recurrent prostate cancer. *Practical Radiation Oncology: An official journal of the American Society for Radiation Oncology* (2023). doi: 10.1016/j.prro.2023.05.007

69. Brennan VS, Burleson S, Kostrzewa C, Godoy Scripes P, Subashi E, Zhang Z, et al. SBRT focal dose intensification using an MR-Linac adaptive planning for intermediate-risk prostate cancer: An analysis of the dosimetric impact of intra-fractional organ changes. *Radiotherapy Oncol* (2023) 179:109441. doi: 10.1016/j.radonc.2022.109441

70. Dang J, Kong V, Li W, Navarro I, Winter JD, Malkov V, et al. Impact of intrafraction changes in delivered dose of the day for prostate cancer patients treated with stereotactic body radiotherapy via MR-Linac. *Tech Innov Patient Support Radiat Oncol* (2022) 23:41–6. doi: 10.1016/j.tipsro.2022.08.005